Influence of Cohesion on Scour at Piers Founded in Clay–Sand–Gravel Mixtures

Rajesh Jain[1]; A. S. Lodhi[2]; Giuseppe Oliveto, M.ASCE[3]; and Manish Pandey, M.ASCE[4]

Abstract: An accurate prediction of scour depth around bridge piers is crucial for economical and safe design of bridge pier foundations. The main objective of the present study is to identify the influencing cohesive parameters and their effects on the local scour processes around bridge piers, depending on various proportions of clay–sand–gravel mixtures. Twenty experimental tests were performed in a channel 25 m long and 1.0 m wide for this purpose. Runs lasted from 16 to 40 h. It was noted from the experimental work that an increment of clay fraction significantly reduces the scour depth around bridge piers. It was also observed that the initiation of scour occurred at the sides of the pier where separation of flow occurred. Typically, the maximum scour depth at the equilibrium stage was still observed at the sides of the pier. A dimensional analysis was used to propose mathematical relationships assessing the temporal scour depth variation at the wake and sides of the pier. The developed relationships yielded reasonable results with maximum error of two folds for 95.22% of total data sets for scour depth at the wake and 92.57% of the total data sets for scour depth at the sides of the pier. **DOI: 10.1061/(ASCE)IR.1943-4774.0001616.**

Author keywords: Bridge pier; Cohesive sediments; Laboratory scour experiments; Sediment transport; Temporal scour depth variation.

Introduction

Scour is recognized as the main cause of bridge failure. Therefore, it is very important to accurately predict the scour depth around piers to determine the depth of foundation for bridges. Scour depth around bridge elements below the bed level in erodible bed streams can vary significantly depending on the diameter of the pier, sediments, and flow characteristics (e.g., Oliveto and Hager 2002, 2005, 2014; Azamathulla et al. 2010; Azamathulla 2012; Pagliara and Palermo 2011; Lodhi et al. 2014; Kurdistani and Pagliara 2017; Singh et al. 2019, 2020; Pandey et al. 2018, 2019, 2020a, b; Parola et al. 1997; Pourshahbaz et al. 2020; Pu et al. 2020). Kothyari (2007) reported that large rivers like the Ganga and Brahmaputra in India should have a great depth of bridge pier foundations up to 50 m below the riverbed. Thus, an accurate estimation of scour depth around bridge piers significantly increases the life of bridges and reduces the cost of construction in bridge foundation designs. Kamojjala et al. (1995) reported that a damage of $15 million occurred in the Upper Mississippi Basin due to abutment and pier failures related to scour. Similarly, in India a number of bridge failures due to scour in the recent past are also reported by Kothyari (2007) and Pandey et al. (2020c).

Studies on bridge scour are mainly focused on the analysis of pier scour in clear-water condition in cohesionless soils because it is supposed to improve the design value. Several studies have been conducted on prediction of the scour depth at bridge piers founded in uniform and nonuniform cohesionless sediments, which is well understood at present. However, the streambed sediment typically consists of cohesionless as well as cohesive soils or a clay–sand–gravel mixture (Kothyari and Jain 2008). Generally, mixtures of sediments containing clay are found in upland streams (Kothyari and Jain 2010a, b; Jain and Kothyari 2009). Type and percentage of clay, moisture content, and drainage conditions play an important role in such types of cohesive sediment mixtures (Lodhi et al. 2016). These factors are responsible for bonding between the sediment and its resistance against erosion or scouring. Due to the variations in properties of cohesive sediments, it is hard to predict the incipient flow conditions and scour depth. Few investigations have been conducted recently to study scour in cohesive soil (e.g., Hosny 1995; Ansari et al. 2002; Lodhi et al. 2016). However, no universal formula is presently available to predict the local pier scour depth in cohesive soil because these studies are considered to be at a very early stage (Ansari et al. 2002). Experimental study on scour around piers founded in cohesive sediment is then challenging due to the difficulty in scaling the properties of the cohesive soils and the related complex erosion characteristics (Ting et al. 2001). Kand (1993), Molinas et al. (1999), Briaud et al. (1999, 2001), Ram Babu et al. (2002), Kho (2004), Brandimarte et al. (2006), and Chaudhuri and Debnath (2013) are among the few researchers investigating the scour depth around bridge piers embedded in cohesive sediment mixtures containing clay, sand, and silt. A study on the prediction of the temporal variation of depth of scour at the wake region of bridge piers embedded in clay–gravel (CG) and clay–sand–gravel (CSG) mixtures was conducted by Kothyari et al. (2014). Findings of some of the previously cited experimental works are briefly described in the following.

Briaud et al. (1999) explored the scour depth around bridge piers embedded in clay and sand. A new approach named SRICOS

[1]Professor, Dept. of Civil Engineering, L.D. College of Engineering, Ahmedabad, Gujarat 380015, India. Email: rajeshjain@ldce.ac.in

[2]Assistant Professor, College of Agriculture, Waraseoni, Balaghat, Madhya Pradesh 481331, India. ORCID: https://orcid.org/0000-0002-6660-7177. Email: ajay0312@gmail.com

[3]Associate Professor, School of Engineering, Univ. of Basilicata, Potenza 85100, Italy. ORCID: https://orcid.org/0000-0002-1318-2988. Email: giuseppe.oliveto@unibas.it

[4]Assistant Professor, Dept. of Civil Engineering, National Institute of Technology Warangal, Warangal, Telangana 506004, India (corresponding author). ORCID: https://orcid.org/0000-0002-4215-5671. Email: mpandey@nitw.ac.in

Note. This manuscript was submitted on January 27, 2021; approved on June 17, 2021; published online on August 14, 2021. Discussion period open until January 14, 2022; separate discussions must be submitted for individual papers. This paper is part of the ***Journal of Irrigation and Drainage Engineering***, © ASCE, ISSN 0733-9437.

(scour rate in cohesive soils) was proposed to compute the scour depth around cylindrical piers by using three different types of clay and one type of sand. They also developed a new erosion function apparatus (EFA) to compute the initial scour rate around the pier using the curve generated by EFA. The proposed model was validated by using laboratory and field observations.

Molinas et al. (1999) carried out experiments to investigate the properties of cohesive sediments affecting local scour at bridge piers by using silt, fine sand, and montmorillonite clay having medium plasticity. In their experimental runs, the intensity of compaction was varied from 58% to 93% and the initial water content in unsaturated and saturated clay was varied from 15% to 20% and 32% to 48%, respectively. The authors observed that the slope of the scour hole in cohesive sediment mixture was steeper than that in cohesionless sediments; the slope became steeper with increasing the amount of compaction. The scour hole slope was observed lower in compacted unsaturated mixtures and was very similar to that in cohesionless sediments. The authors also found that the scour hole volume decreased with increasing the compaction and initial water content of the soil. Saturated mixtures with low initial water content offered high resistance to erosion.

Ting et al. (2001) performed laboratory tests on pier scour in clay–sand beds and found that the maximum scour depth and the scour hole shape mainly depend on the pier Reynolds number.

Ansari et al. (2002) studied the influence of cohesion on pier scour. They used clay–sand mixture as cohesive sediment in their experiments. They showed the variation of d_{cpm}/d_{pm} with W/W_{r*} and C_*/ϕ_*, where d_{cpm} is the maximum scour depth around pier in cohesive sediment, d_{pm} is the maximum scour depth around pier in cohesionless sediment, W is the antecedent moisture content, W_{r*} is the moisture content required to saturate the soil sample, C_* is the dimensionless cohesion, and ϕ_* is the dimensionless angle of internal friction for cohesive sediment mixture. It was found that the d_{cpm}/d_{pm} initially decreased with an increase in W/W_{r*} up to 1.0; thereafter, it started increasing with further increase in W/W_{r*}. The authors also found that the rate of erosion was least when W/W_{r*} approaches unity and plasticity index $(\mathrm{PI}) > 0$. It was also concluded that the scour depth in plastic sediments reduces with an increase in C_*/ϕ_*. Here the parameter C_*/ϕ_* represents the cohesion strength of the sediment mixture. In a subsequent study, Ansari et al. (2003) analyzed the effect of cohesion experimentally. They found that the maximum scour depth occurs either at the sides of the pier or downstream of the pier depending on clay properties.

Brandimarte et al. (2006) developed a methodology to study the scour risk to bridge foundations in cohesive soils. The proposed methodology was applied to the Woodrow Wilson Bridge on the River Potomac in Washington, DC. The sediment deposits in the river mainly consisted of soft clay, silt, and silty sand. The proportion of soil (particles less than 0.06 mm) varied from 48% to 71%, and the plasticity index varied from 33% to 41%. The scour depth in cohesive soils was estimated by the method proposed by Briaud et al. (2001), according to whom the scour process in cohesive soils would occur at a slow rate.

Debnath and Chaudhuri (2010a, b) conducted experimental investigations on local scour around cylinders founded in a cohesive sediment bed. It was observed that the scour depth decreases with an increase in clay content for a clay–sand mixture containing less than 24% water content. For the same mixture containing water content greater than 27%, the maximum scour depth decreases with increasing the clay content by up to 50%–70%; thereafter it increases. It was also observed that the clay content in clay–sand mixture significantly reduces the peripheral expansion and depth of the scour hole.

Dey et al. (2011) presented the results of an experimental investigation on scour around vertical piles founded in clay and clay–sand mixture beds under waves. They stated that the scour depth reduces with an increase of clay content in clay–sand mixture. Barbhuiya and Chakma (2012) concluded that the maximum scour depth at equilibrium condition decreases with increasing in dry density of silt and clay content.

Link et al. (2013) completed a laboratory experimental study to quantify the effect of bed compaction on scour depth around piers embedded in sand–clay mixtures. They observed that the sediment was scoured in a particle-by-particle and/or aggregate-by-aggregate manner and in the form of chunks of aggregate. The maximum scour depth occurred at the wake of the pier with an increase in the ratio of actual to Proctor's optimum molding water content ($\hat{w}$). It was observed that the depth of scour decreased with increasing water content ($\hat{w}$) up to 2.5, whereas in case of $\hat{w}>2.5$, the scour depth increased with increasing water content.

Kothyari et al. (2014) conducted several experiments to calculate the scour depth in the wake region of a circular pier founded in CG and CSG sediment mixtures. Clay had median grain size of 0.052 mm and $\mathrm{PI} = 6.16\%$. It was found that the unconfined compressive strength of sediment and fraction of clay significantly influence the scour depth.

Keeping the earlier research in view, it can be concluded that all the available investigations have been carried out to study scour depth at piers fixed in clay or clay–sand mixtures. Contrarily, the present study aims to assess the temporal scour depth variation around bridge piers at the sides and the wake embedded in CG and CSG sediment mixtures. It is necessary to assess the temporal variation of the scour depth at the sides of bridge piers in addition to scour depth at the wake of bridge pier. Hence, the present study has been taken up. It is also important to note that Kothyari et al. (2014) studied the scour depth only at the wake region of bridge piers founded in CG and CSG sediment mixtures; however, they used mobile beds with low plastic clay content with clay percentage beginning from 20% in mixtures. Further novelties of this study are the presentation of new experimental data for cohesive soils obtained from runs of duration from 16 to 40 h and the proposal of a new approach for the temporal scour depth variation in cohesive soil. This approach has the advantage to be linked (thus constituting a generalization) to that by Kothyari et al. (2007) for cohesionless bed sediments.

Experimental Setup and Procedure

Experimental Flume

Extensive experimental tests were carried out to study the influence of cohesion on development of scour and scour depth around circular piers founded in CG and CSG sediment mixtures at the Hydraulic Engineering Laboratory of the Civil Engineering Department at the Indian Institute of Technology in Roorkee, Uttarakhand, India. A rectangular flume having length of 25 m, width of 1 m, and depth of 0.6 m was used for the tests. All experiments were carried out on two bed slopes of flume, that is, 3×10^{-3} and 5×10^{-3}. The working section of flume had length of 4 m, width of 1 m, and depth of 0.6 m, starting at 12 m downstream from the flume entrance. Therefore, the approach flow was a fully developed flow. The flow rate in the flume was regulated by an overhead tank by maintaining a constant head. A tail gate was provided downstream of the flume to regulate the approach flow depth. An ultrasonic flow meter at the inlet pipe of the flume was used to measure the continuous flow discharge. The approaching

flow depth and scour depth were measured by a vertical point gauge (1.2 m in length graduated to centimeters and millimeters) with a flat bottom having an accuracy of 0.1 mm. The flat bottom point gauge was used to avoid the penetration of gauge in the scoured bed while measuring the scour depth. Enough care was taken while measuring the scour depth. The flat bottom gauge was lowered very slowly into the water such that it did not disturb the flow and compacted sediment bed conditions. Also, the approach flow depth was measured 4 m upstream of the cylindrical pier in order to avoid any influence of pier in the observation of flow depth. Two sizes of cylindrical iron pipes having outer diameters of 11.52 and 8.90 cm were used in the experiments. The surfaces of the pipes were painted to give a smooth finish.

Sediment Material

The experimental beds were prepared with the use of fine gravel, fine sand, and clay having median size (d_{50}) of 2.7, 0.24, and 0.0014 mm, respectively. The geometric standard deviations of the clay, sand, and gravel were 2.16, 1.41, and 1.21, respectively. The other properties of clay were cohesion at optimum moisture content (C_u) = 49.23 kN/m^2, angle of friction at optimum moisture content (φ_c) = 30.7°, plastic limit (PL) = 22%, liquid limit (LL) = 43%, plasticity index (PI) = 21%, optimum moisture content (OMC) = 19%, maximum dry density $(\gamma_d)_{\max}$ = 16.43 kN/m^3, and relative density 2.65. X-ray diffraction (XRD) tests were conducted to determine the mineralogical properties of clay, showing minerals percentages in the clay: montmorillonite = 4.5%, kaolinite = 18%, and illite = 77.5%.

Preparation of Cohesive Sediment Bed Mixtures

Two types of sediment mixtures (i.e., CG and CSG) were considered in this study. For the preparation of the mobile beds, powdered clay, sand, and fine gravel sediments were used in various proportions. As an example, for the preparation of CG mixture beds, clay was mixed to gravel in percentages ranging from 10% to 50% by weight. Similarly, for the preparation of CSG mixture beds, clay was mixed with sand and gravel in percentages ranging from 10% to 50% by weight. In CSG mixture beds, the ratio of sand and gravel was kept equal by weight. The chosen ratio of ingredients was used in preparation of CG and CSG mixtures in order to avoid any calculation error. After being accurately weighed all three sediments were mixed thoroughly. Clear water was mixed into the mixture and the three sediments mixed homogeneously again. The prepared mixtures were covered with plastic sheets for 24 h to allow uniform moisture distribution. They were again mixed properly before placing of sediment mixtures into the working section. The working section was completely filled with prepared sediment mixture, and a pier model was fixed at the center of the working section. This sediment mixture was compacted in three different layers having 0.10 m thickness, approximately, using a dynamic compaction method. All of that was completed using a cylindrical roller of 0.23 m diameter, 0.63 m length, and dead weight of 100 N. This approach was effectively applied by Robinson and Hanson (1995), Hanson and Hunt (2006), Jain and Kothyari (2009), Kothyari et al. (2014), and Lodhi et al. (2016, 2018). The area around the sides of the channel and pier was compacted using a wooden hand hammer having dimensions of 0.40 m length, 0.10 m width, and 0.07 m thickness. A sharp-edged trowel was used to remove the extra sediment from the bed surface. The final thickness of prepared sediment mixture in the working section was kept at approximately 30 cm.

For the measurements of antecedent unconfined compressive strength, dry density, and moisture content, three samples were taken randomly from different locations to ensure the uniform compaction of sediment mixture. Before starting of each experiment, the prepared sediments mixture bed was left saturated for 24 h. A Perspex sheet of 2.5 mm thickness was used to cover the sediment bed around the pier to avoid inception of scour before the flow attains predefined conditions in the flume.

All the experiments were conducted in two phases, namely (1) with cohesionless sediment (gravel and gravel–sand mixture); and (2) with cohesive sediment mixtures CG and CSG. Experiments with cohesionless sediment beds are not described in this paper for brevity. A total of 20 experimental runs were completed with cohesive sediment mixtures on pier scour. In the present investigation, an approach described in Lodhi et al. (2016, 2018) for the quantification of the influence of cohesion on scouring around spur dikes was followed. The experiments were conducted in two series, viz., (a) clay was varied from 10%–50% and mixed with fine gravel; and (b) clay was varied from 10%–50% and mixed with equal amounts of fine gravel and fine sand, by weight. A total of 350 temporal scour depths were taken at pier sides, out of which 186 observations were taken in CG mixture beds and 164 observations were taken in CSG mixture beds. A total of 335 temporal scour depths were taken at the wake of the pier, out of which, 177 observations were taken in CG and 158 observations in CSG mixture beds. A summary of the experimental tests is presented in Table 1. Approximately 16 scour depths were measured in each run. The scour depths were measured over shorter time intervals during the initial part of the experimental run when the scour process were taking place at a rapid rate. However, scour depths were measured over larger time intervals in the later part of the run. Similar to Kothyari et al. (2014), the runs were carried out until equilibrium scour condition was reached (after which scour depth did not change with time). For this study, all experiments were reached equilibrium after runs from 26 to 40 h. The number of observations is different in CG and CSG mixtures because the time to obtain semi-equilibrium conditions was different in both mixtures. It is worth noting that the definition of the equilibrium condition for cohesive soil is different from the typical ones for cohesionless bed sediments, as argued by Mazurek (2001) and Hamidifar and Omid (2017). However, this study would like to prescind from equilibrium conditions, considering the processes of temporal scour depth variation. Moreover, the timescale for scouring in cohesive sediments was different from that of noncohesive sediments. The timescale for scouring in cohesive sediments was also varied with the percentage of clay in sediment bed. In general, the duration of experimental run (when depth of scour did not change appreciably with time) increased with clay percentage. The ranges for the measured experimental data and flow conditions are presented in Tables 2 and 3 for CG and CSG mixtures, respectively.

Dimensional Considerations

Previous studies on pier scour in cohesionless sediment show that scour depth depends mainly on characteristics of flow, sediment, and pier diameter, whereas clay fraction, dry density, and unconfined compressive strength were recognized as the most influential parameters for cohesive sediment beds (Molinas et al. 1999; Jain and Kothyari 2010; Kothyari et al. 2014). It is difficult to investigate the influence of such parameters through analytical methods. Therefore, such variation in scour depth is studied using dimensional analysis here. Experiments were conducted on vertical circular piers only. However, further effects of the type pier shape,

Table 1. Summary of the experimental runs on scour in CG and CSG mixtures

No.	Run no.	Clay (%)	Sand (%)	Gravel (%)	Pier diameter (m)	No. of observations at wake of the pier	No. of observations at side of the pier	Duration of experimental run (h)
1	CG1.1	10	—	90	0.1152	16	16	18
2	CG1.2	10	—	90	0.0890	15	16	18
3	CG2.1	20	—	80	0.1152	19	21	30
4	CG2.2	20	—	80	0.0890	17	18	26
5	CG3.1	30	—	70	0.1152	22	24	40
6	CG3.2	30	—	70	0.0890	14	15	24
7	CG4.1	40	—	60	0.1152	19	20	40
8	CG4.2	40	—	60	0.0890	19	20	40
9	CG5.1	50	—	50	0.1152	18	18	40
10	CG5.2	50	—	50	0.0890	18	18	40
11	CSG1.1	10	45	45	0.1152	14	14	16
12	CSG1.2	10	45	45	0.0890	14	14	16
13	CSG2.1	20	40	40	0.1152	17	18	26
14	CSG2.2	20	40	40	0.0890	16	17	26
15	CSG3.1	30	35	35	0.1152	18	18	30
16	CSG3.2	30	35	35	0.0890	14	17	30
17	CSG4.1	40	30	30	0.1152	16	16	30
18	CSG4.2	40	30	30	0.0890	16	16	30
19	CSG5.1	50	25	25	0.1152	17	17	40
20	CSG5.2	50	25	25	0.0890	16	17	40

Table 2. Experimental conditions for pier scour founded in CG mixtures

Run number	P_c (%)	d_a (mm)	W (%)	γ_d (kN/m^3)	UCS (kN/m^2)	e	h (m)	U_o (m/s)	S_o	D (m)	d_{cps} (m)	d_{cpw} (m)	T (min)
CG1.1	10	2.431	5.76	13.08	0.00	0.99	0.121	0.573	0.003	0.1152	0.124	0.083	1,800
CG1.2	10	2.431	5.46	12.76	0.00	1.04	0.117	0.593	0.003	0.089	0.101	0.076	1,800
CG2.1	20	2.163	8.09	15.78	3.68	0.65	0.114	0.716	0.003	0.1152	0.101	0.065	1,800
CG2.2	20	2.163	7.49	15.49	2.92	0.68	0.113	0.722	0.003	0.089	0.080	0.049	1,560
CG3.1	30	1.894	9.14	16.18	9.08	0.61	0.115	0.760	0.003	0.1152	0.087	0.049	2,400
CG3.2	30	1.894	8.18	16.41	9.14	0.58	0.113	0.774	0.003	0.089	0.030	0.013	1,440
CG4.1	40	1.626	11.97	17.93	15.68	0.45	0.125	0.704	0.005	0.1152	0.050	0.037	2,400
CG4.2	40	1.626	12.82	18.10	16.11	0.44	0.115	0.765	0.005	0.089	0.034	0.025	2,400
CG5.1	50	1.357	17.36	16.71	14.06	0.56	0.087	1.011	0.005	0.1152	0.041	0.034	2,400
CG5.2	50	1.357	17.30	16.76	14.60	0.55	0.087	1.011	0.005	0.089	0.029	0.020	2,400

Note: Here P_c = percentage of clay; d_a = weighted arithmetic mean size of the mixtures of cohesive sediment; W = antecedent moisture content; γ_d = dry density; UCS = unconfined compressive strength; e = void ratio; h = approaching flow depth; U_o = approaching flow velocity; S_o = bed slope; D = pier diameter; d_{cps} = scour depth at the sides of the pier at the time T in the last column; d_{cpw} = scour depth at the wake of the pier at the time T in the last column; T = experimental run time; and CG = mixture of cohesive sediment containing clay and gravel.

Table 3. Experimental conditions for pier scour founded in CSG mixtures

Run number	P_c (%)	W (%)	d_a (mm)	γ_d (kN/m^3)	UCS (kN/m^2)	h (m)	U_o (m/s)	e	S_o	D (m)	d_{cps} (m)	d_{cpw} (m)	T (min)
CSG1.1	10	8.37	1.324	17.34	0.00	0.119	0.534	0.50	0.003	0.1152	0.140	0.111	960
CSG1.2	10	8.99	1.324	17.54	0.00	0.118	0.538	0.48	0.003	0.089	0.122	0.094	960
CSG2.1	20	10.19	1.179	18.34	11.30	0.122	0.614	0.42	0.003	0.1152	0.107	0.051	1,560
CSG2.2	20	9.63	1.179	17.78	11.08	0.127	0.589	0.46	0.003	0.089	0.085	0.039	1,560
CSG3.1	30	10.44	1.033	18.80	36.33	0.117	0.780	0.38	0.003	0.1152	0.056	0.041	1,800
CSG3.2	30	11.09	1.033	19.61	41.09	0.116	0.786	0.33	0.003	0.089	0.034	0.030	1,800
CSG4.1	40	11.81	0.888	19.07	54.07	0.101	0.844	0.36	0.005	0.1152	0.032	0.032	1,800
CSG4.2	40	11.45	0.888	18.50	51.47	0.087	0.980	0.40	0.005	0.089	0.025	0.019	1,800
CSG5.1	50	13.61	0.742	18.27	52.34	0.099	0.861	0.42	0.005	0.1152	0.028	0.025	2,400
CSG5.2	50	13.88	0.742	18.39	53.09	0.080	1.066	0.41	0.005	0.089	0.020	0.018	2,400

Note: Here P_c = percentage of clay; d_a = weighted arithmetic mean size of the mixtures of cohesive sediment; W = antecedent moisture content; γ_d = dry density; UCS = unconfined compressive strength; e = void ratio; h = approaching flow depth; U_o = approaching flow velocity; S_o = bed slope; D = pier diameter; d_{cps} = scour depth at the sides of the pier at the time T in the last column; d_{cpw} = scour depth at the wake of the pier at the time T in the last column; T = experimental run time; and CSG = mixture of cohesive sediment containing clay, sand, and gravel.

pier inclination, and pier foundation might be considered with approaches similar to those used by Oliveto and Hager (2002) for the calculation of the scour depth around bridge piers founded in uniform and nonuniform cohesionless sediments. Scour depth around a bridge pier founded in a loose material, obtained from laboratory experiment, has an inherent scale effect. Consideration of the scale effect leads to a consistent set of nondimensional parameters needed to describe the influences of flow, bed sediment, and pier variables (Ettema et al. 1998). Debnath and Chaudhuri (2010a, b) and Kothyari et al. (2014) stated that the scour depth around bridge piers in cohesive sediment beds is mainly influenced by

$$d_c = f_1(P_c, C_u, d_a, \phi_c, \phi_{sh}, \gamma_d, \gamma_w, \gamma_s, UCS, u, T, d_s) \quad (1)$$

where d_c = instantaneous scour depth in cohesive sediment; P_c = clay percentage; C_u = cohesion of pure clay; d_a = weighted arithmetic diameter of prepared CG and CSG mixture; ϕ_{sh} = internal friction angle for cohesionless sediment; ϕ_c = internal friction angle for clay; γ_d = dry density; γ_s = specific weight of sediment; γ_w = specific weight of water; UCS = unconfined compressive strength; u = approach flow velocity; T = time parameter; and d_s = instantaneous depth of scour in cohesionless sediment under similar flow conditions. In this study, d_s is calculated as done by Kothyari et al. (2007). The effect of shear stress on pier scour is implicitly accounted for when the computation of scour depth in cohesionless sediment (d_s) is considered. In order to calculate the value of d_a, the procedure outlined by Jain and Kothyari (2009, 2010) and Lodhi et al. (2016, 2018) was utilized.

The variables C_u, ϕ_c, ϕ_{sh}, UCS, and T can be written in dimensionless form as follows (Kothyari et al. 2014; Lodhi et al. 2016, 2018):

$$C_* = \frac{P_c C_u}{(\gamma_s - \gamma_w) d_a} \quad (2)$$

$$\phi_* = \frac{P_c \tan\phi_c + (1 - P_c)\tan\phi_{sh}}{\tan\phi_{sh}} \quad (3)$$

$$UCS_* = \frac{UCS}{(\gamma_s - \gamma_w) d_a} \quad (4)$$

$$t_* = T\left(\frac{u}{d_a}\right) \quad (5)$$

where C_* = cohesion in dimensionless form; ϕ_* = dimensionless friction angle for cohesive sediment mixture; UCS_* = dimensionless unconfined compressive strength of CG and CSG sediment mixtures; and t_* = dimensionless time. It is necessary to mention here that C_u indicates the cohesion of pure clay. Clay is added in various proportions in gravel and sand–gravel mixtures in this investigation. The cohesion value of various CG and CSG mixtures was obtained by introducing P_c in Eq. (2).

Thus, Eq. (1) can be rewritten as

$$d_c = f_2(d_s, P_c, C_*, \phi_*, \gamma_d, \gamma_w, UCS_*, t_*) \quad (6)$$

Using Buckingham's π theorem (Peerless 1967) and dimensional analysis (Jain and Kothyari 2009, 2010) amongst various variables, the variables of Eq. (6) are rearranged in dimensionless form as

$$\frac{d_c}{d_s} = f_3\left(P_c, \frac{C_*}{\phi_*}, \frac{\gamma_d}{\gamma_w}, UCS_*, t_*\right) \quad (7)$$

The value of γ_d/γ_w was varied from 1.30 to 2.0. The analysis of such variable with scour depth showed that the variation of γ_d/γ_w was nonsignificant to completely elucidate the variation in scour depth. This result was very similar to outcomes found by Kumar (2011) and Kothyari et al. (2014) during the analysis of impact of such variables on depth of scour around the pier embedded in cohesive sediment beds. Also, Jain and Kothyari (2009, 2010) found similar influence of γ_d/γ_w on suspended load and bed load transport during detachment of cohesive sediment mixtures like CSG and CG. Hence, this variable was neglected from further analysis and Eq. (7) can be reconsidered as follows:

$$\frac{d_c}{d_s} = f_4\left(P_c, \frac{C_*}{\phi_*}, UCS_*, t_*\right) \quad (8)$$

Eq. (8) was used to compute the scour depth around bridge piers founded in cohesive sediment mixtures. The value of d_s in Eq. (8) was calculated by the relationship proposed by Kothyari et al. (2007) for the calculation of the scour depth around bridge piers founded in uniform and nonuniform cohesionless sediments. This relationship relates the temporal variation of the scour depth to the difference between the actual and the entrainment densimetric particle Froude number, i.e., $(F_d - F_{d\beta})$, considering a large number of data sets from several laboratory experiments. The authors proposed the following equation:

$$d_* = d_s/z_R = 0.272\sigma_g^{-1/2}(F_d - F_{d\beta})^{2/3}\log T \quad (9)$$

where $F_{d\beta}$ for scour inception around bridge piers is defined as

$$F_{d\beta} = \left[F_{di} - 1.26 \cdot \beta^{1/4} \cdot \left(\frac{R_h}{d_a}\right)^{1/6}\right]\sigma_g^{1/3} \quad (10)$$

F_{di}, which is the densimetric particle Froude number for incipient sediment entrainment in the approach flow channel, is, in turn, defined as

$$F_{di} = 2.33 D_*^{-0.25}\left(\frac{R_h}{d_a}\right)^{1/6} \quad \text{for } D_* \le 10 \quad (11)$$

$$F_{di} = 1.08 D_*^{1/12}\left(\frac{R_h}{d_a}\right)^{1/6} \quad \text{for } 10 < D_* < 150 \quad (12)$$

$$F_{di} = 1.65\left(\frac{R_h}{d_a}\right)^{1/6} \quad \text{for } D_* \ge 150 \quad (13)$$

Here d_* = dimensionless maximum scour depth; d_s = instantaneous scour depth in cohesionless sediment; z_R = reference length = $(hD^2)^{1/3}$ for cylindrical pier; h = approach flow depth; σ_g = sediment gradation; T = time parameter; R_h = hydraulic radius; and D_* = dimensionless sediment particle size. Specifically, $D_* = (g'/\nu^2)^{1/3} d_a$ with $g' = [(\gamma_s - \gamma_w)/\gamma_w]g$ = relative gravitational acceleration and g = gravitational acceleration.

Results and Discussion

Visual Analysis

Scour patterns around the bridge piers at 10% clay content in both types of sediment mixture (i.e., CG and CSG) were very similar to those in cohesionless sediment. Significant scour occurred at the nose of the bridge pier, and the morphology of the scour hole was cone-shaped. The maximum scour depth was observed at the nose of the bridge pier in both types of cohesive sediment mixture

containing 10% clay content. Conversely, no scour depth was observed at the nose of the pier when clay percent was varied from 20% to 50% in both types of sediment mixture for all experiments. In such conditions the maximum scour depth was observed at the sides of the pier.

At lower percentages of clay (≤20%), scour started with the removal of particles around the pier. At higher percentages of clay, sediment was detached in the form of thick flakes from the bed surface. For certain runs with higher values of *UCS* and higher percentages of clay (>40%), sediment detachment took place in the form of chunks. Ansari et al. (2002) and Kothyari et al. (2014) observed similar erosion patterns in case of clay-sand and clay–sand–gravel mixtures, respectively. Also, Mazurek et al. (2001) observed similar erosion patterns in the case of scour caused by submerged circular turbulent impinging jets in clay–sand mixtures.

All experiments were conducted under clear-water conditions on CG and CSG mixture beds. No sediment deposition was observed at the wake of the pier, whereas significant deposition of sediment was observed when experiments were conducted with cohesionless sediment beds. Different scour hole shapes were observed in CG [Figs. 1(a and b)] and CSG [Figs. 2(a and b)] sediment mixtures. Scour patterns in these sediments were thus drastically different from those noticed for cohesionless sediments. The shape of the scour hole changed with increasing the clay content in the sediment bed. In particular, the resistance to erosion increased with increasing clay content in the bed, which affected the shape of the scour hole developed under various clay percentages of CG and CSG mixtures. Comparatively, larger scour depths were observed in CG mixtures [Fig. 1(b)] than in CSG mixtures [Fig. 2(a)] for the same clay content. It is evident from Table 2 that CSG mixtures have greater values of *UCS* than those of CG mixtures. Larger scour depths in CG mixtures might be attributed to the lower resistance offered against erosion owing to lesser *UCS* values.

Influence of Clay Content and Unconfined Compressive Strength on Scour Depth

Figs. 3–6 were prepared to investigate the influence of clay content and unconfined compressive strength of the cohesive sediment mixtures on the scour depth at the side (d_{cps}) and the wake (d_{cpw}) of the pier. It is evident from the figures that the scour depth reduces with increasing clay content and unconfined compressive strength in the sediment bed. In other terms, the resistance ability of cohesive sediment mixtures to the erosion increases with increment of clay content and *UCS* (Jain and Kothyari 2010). Here, it is noteworthy that the scour depth reduced significantly in CSG mixtures rather than in CG mixtures for clay content ≥20% (Figs. 3 and 5). Similar results were also observed by Lodhi et al. (2016, 2018) in the case of experiments on variation of temporal depth of scour around submerged and partially submerged spur dikes. In Figs. 4 and 6 scour processes initiated very late for the experiments with larger values of *UCS* owing to the greater resistance against erosion. The shear stress is not large enough in comparison to the resistance of bed sediment owing to larger values of *UCS* (Kothyari et al. 2014).

Variation of Temporal Scour Depth around Piers

To quantify the scour depth around circular piers founded in cohesive sediments in comparison to those of cohesionless sediments of similar bulk characteristics, Figs. 7–10 were prepared. Experimental data of the present study were used to this purpose for various proportions of clay content in CG and CSG sediment mixtures. In Figs. 7 and 8, the instantaneous maximum depths of scour (d_{sp}) were computed using Kothyari and colleagues' (2007) approach by considering CG and CSG mixtures to be cohesionless, whereas d_{cps} and d_{cpw} are the instantaneous observed scour depths at the sides and the wake of pier in cohesive sediment mixtures bed, respectively. It is worth noting that the Kothyari and colleagues' (2007) approach refers to the maximum scour depth at a given time regardless where it occurs. It can be observed from these figures that scour depths in cohesive sediments were much smaller than those calculated by considering sediments as cohesionless. However, Figs. 7 and 8 indeed revealed that scour depth was drastically different in cohesive sediment mixtures. Under similar flow conditions scour depths in cohesive sediments are significantly smaller than those of sediments with equivalent grain sizes, but in absence of cohesion. In these figures the ratio of $\frac{d_{sp}}{d_{cp}} = 1$ indicates scour

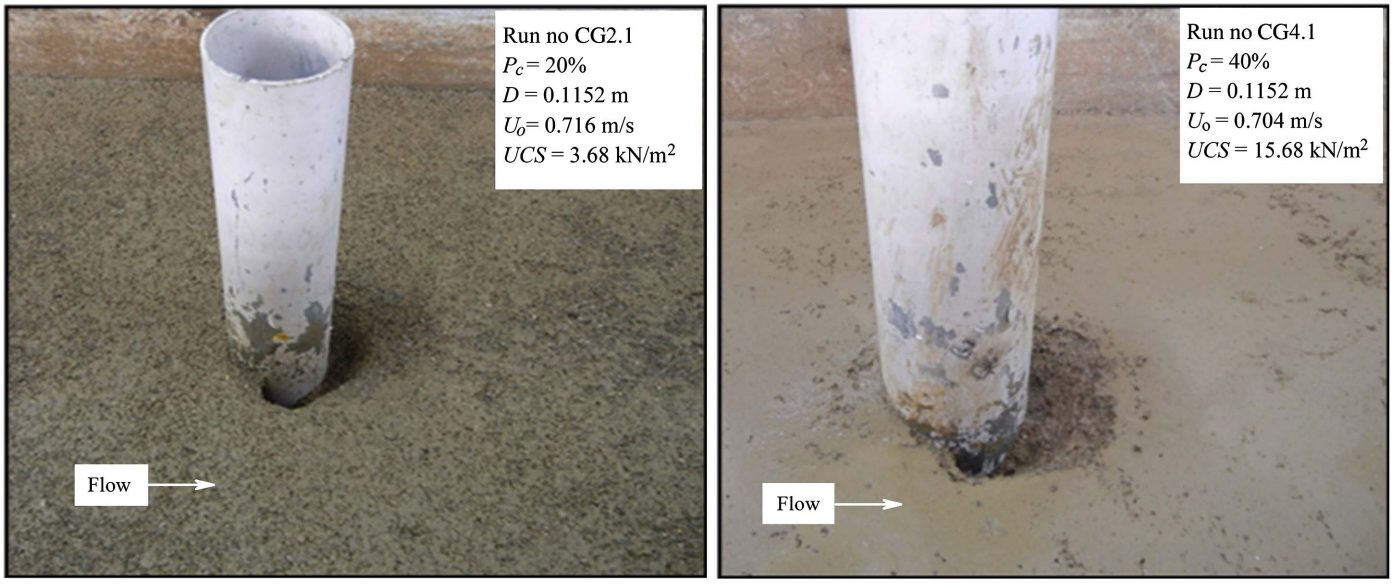

Fig. 1. (a) Scour hole patterns around bridge piers in CG mixtures (Run CG2.1); and (b) scour hole patterns around bridge piers in CG mixtures (Run CG4.1).

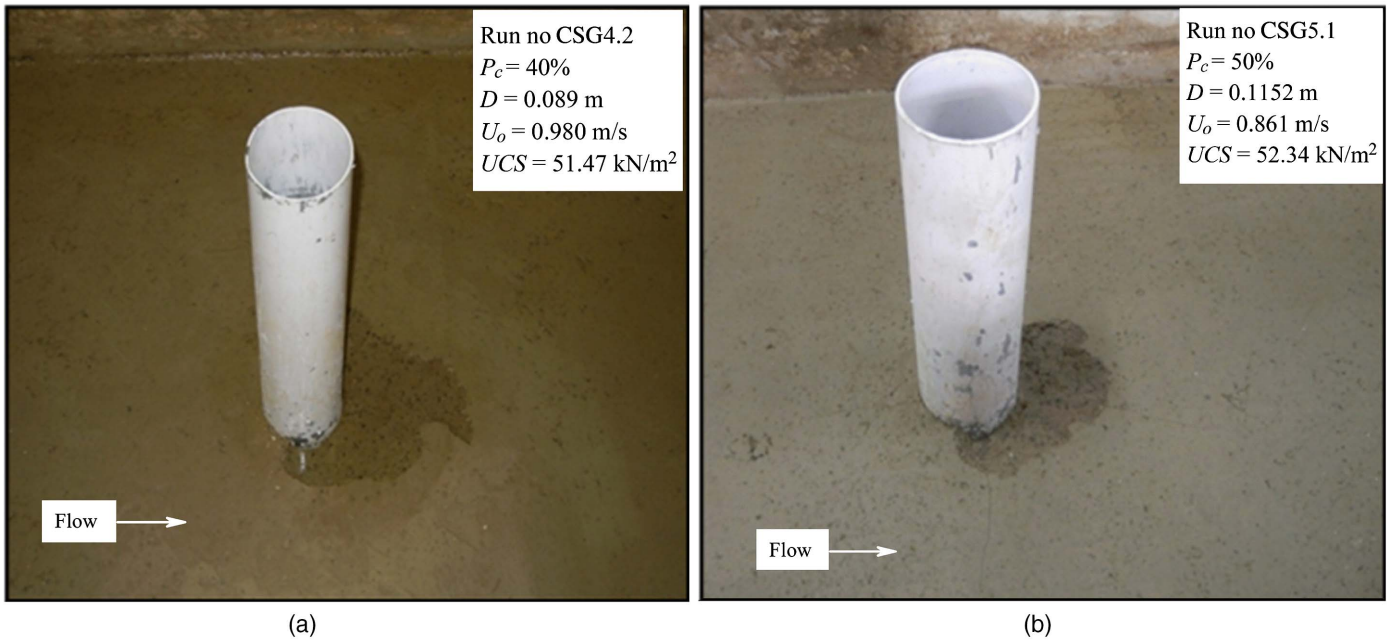

Fig. 2. (a) Scour hole patterns around bridge piers in CSG mixtures (Run CSG4.2); and (b) scour hole patterns around bridge piers in CSG mixtures (Run CSG5.1).

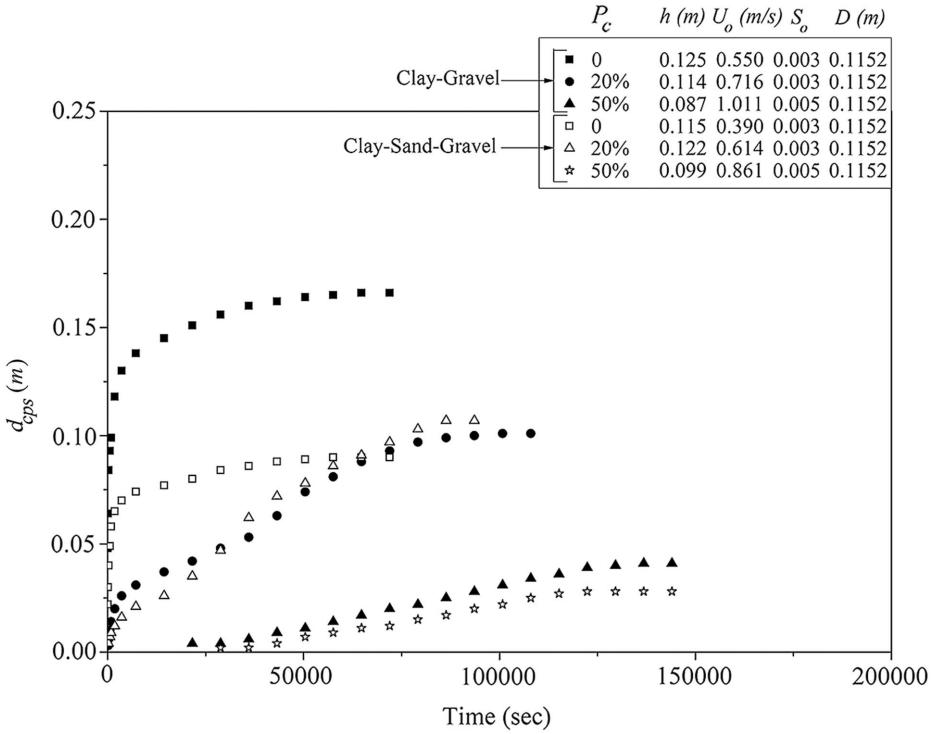

Fig. 3. Scour depth variation with time at the sides of the pier for different clay percentages in CG and CSG sediment mixtures.

depth in cohesionless sediment under the same flow conditions. It is also evident from these figures that the scour depth reduces drastically when clay content is more than 30%. Hence, the whole data sets have been analyzed for two ranges clay of percentages, that is, 10%–20% and 30%–50% to incorporate its effect.

Analogously, Figs. 9 and 10 show the temporal variation of scour depths at the wake of the pier for various unconfined compressive strengths. The whole set of data was classified in three ranges of *UCS* for both types of sediments mixture. It was observed that the *UCS* of the sediment mixtures increases with increasing clay percentage in sediment mixture; hence, it increases the resistance ability of sediment bed against scour. Similar results were reported by Robinson and Hanson (1995) in the context of head cut erosion testing of clay–silt–sand mixtures

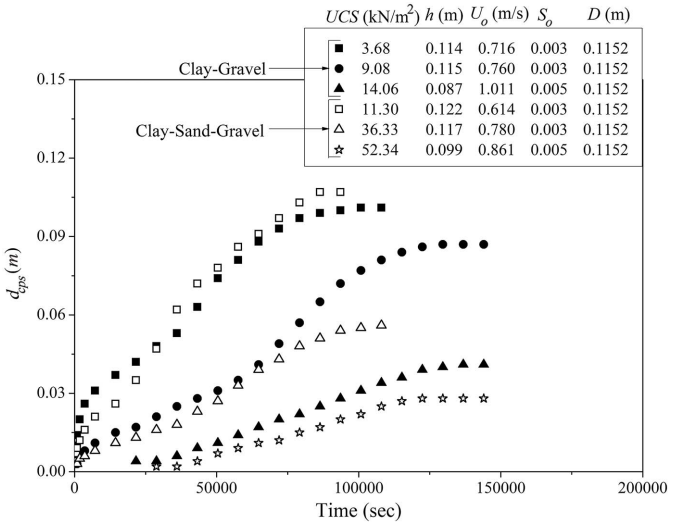

Fig. 4. Scour depth variation with time at the sides of the pier for different unconfined compressive strengths in CG and CSG sediment mixtures.

and by Jain and Kothyari (2009, 2010) in the context of erosion of CG and CSG sediment mixtures.

Therefore, the functional relationship for the computation of scour depths at the sides and the wake of piers founded in CG and CSG sediment mixtures can be rewritten here as

$$\frac{d_{cp(s/w)}}{d_{sp}} = f\left(P_c, \frac{C_*}{\phi_*}, UCS_*, t_*\right) \tag{14}$$

It is necessary to mention here that shear strength parameters C_u and ϕ_c were determined for pure clay only and appropriate weightage was given by multiplying cohesion with clay percentage for various CG and CSG mixtures. Therefore, the variable C_*/ϕ_* could not elucidate the variation in scour depth clearly. This finding was in harmony with the results by Kothyari et al. (2014) in the case of scour at the wake of piers and by Lodhi et al. (2016, 2018) in the case of scour around submerged and partially submerged dikes founded in CG and CSG sediment mixtures. Therefore, the variable C_*/ϕ_* was also removed from further analysis. It is important to replace P_c and UCS_* with $(1 + P_c)$ and $(1 + UCS_*)$ so that Eq. (14) also applies to cohesionless sediment (i.e., $P_c = 0$) (Jain and Kothyari 2009, 2010; Kothyari et al. 2014) and then Eq. (14) can be rewritten as follows:

$$\frac{d_{cp(s/w)}}{d_{sp}} = f[(1 + P_c), (1 + UCS_*), t_*] \tag{15}$$

Finally, the functional relationship in Eq. (15) is used to compute the scour depth at the sides and the wake of the pier founded in CG and CSG sediment mixtures.

Nonlinear multiple regression analysis of all pertinent dimensionless parameters was carried out by Statistica version 8.0 software and the following new relationships are proposed.

For scour depths at the sides of the pier it was found that

$$\frac{d_{cps}}{d_{sp}} = F_{ps} \tag{16a}$$

where F_{ps} = functional cohesion parameter for CG and CSG sediment mixtures, which is given by

$$F_{ps} = \mathrm{m}_o[(1 + P_c)^{m_1}(1 + UCS_*)^{m_2}(t_*)^{m_3}] \tag{16b}$$

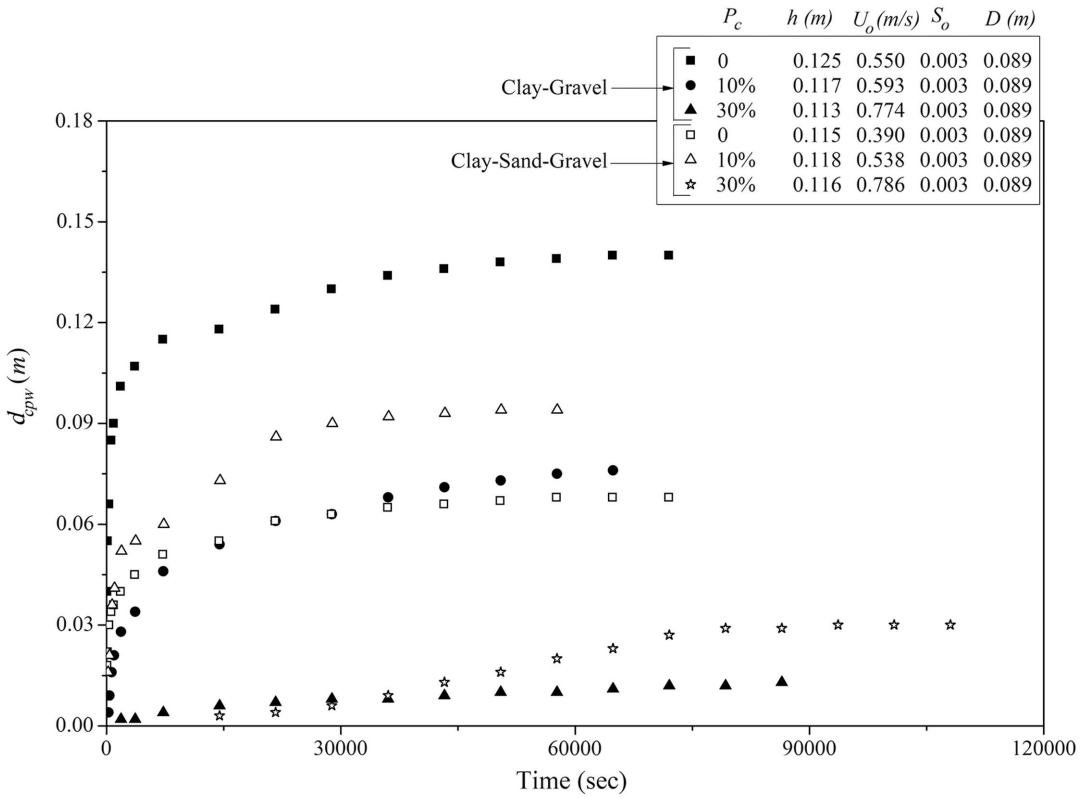

Fig. 5. Scour depth variation with time at the wake of the pier for different clay percentages in CG and CSG sediment mixtures.

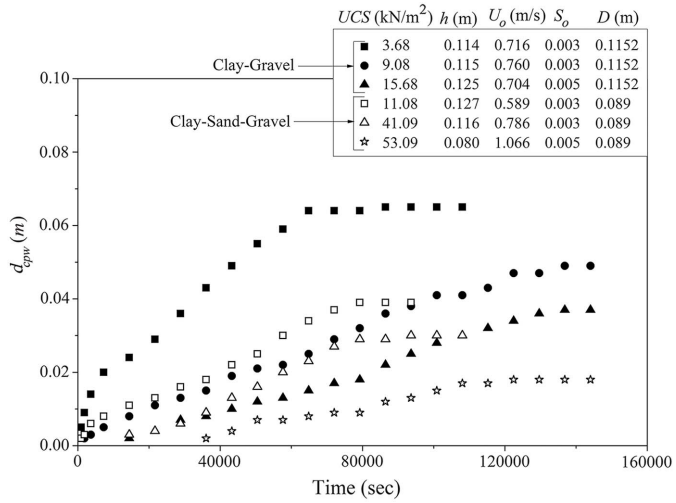

Fig. 6. Scour depth variation with time at the wake of the pier for different unconfined compressive strengths in CG and CSG sediment mixtures.

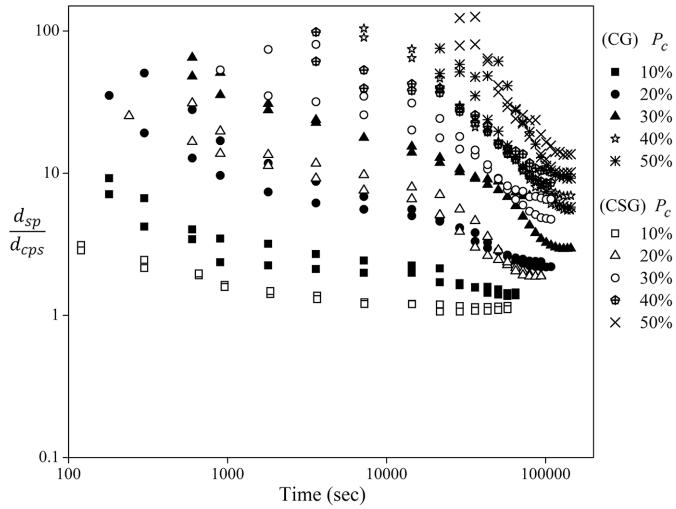

Fig. 7. Temporal variation of dimensionless scour depth at the sides of the pier in CG and CSG sediment mixtures for different percentages of clay content.

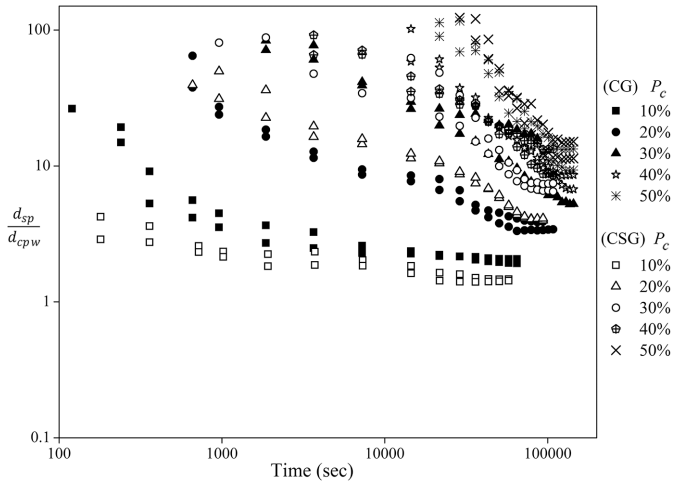

Fig. 8. Temporal variation of dimensionless scour depth at the wake of the pier in CG and CSG sediment mixtures for different percentages of clay content.

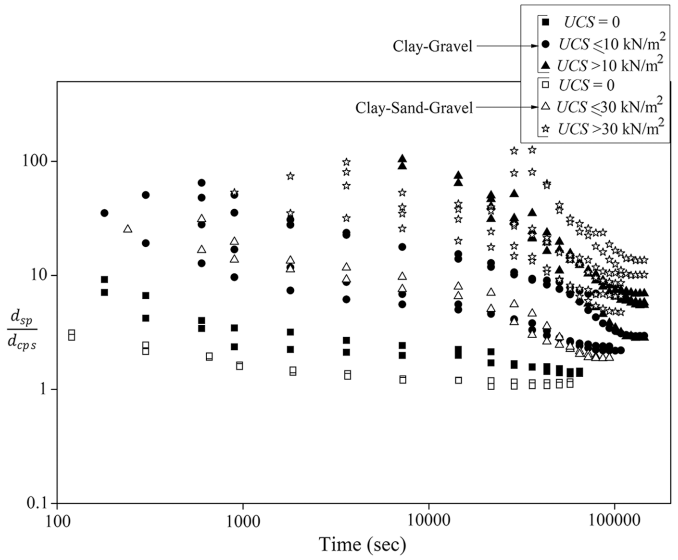

Fig. 9. Temporal variation of dimensionless scour depth at the sides of the pier in CG and CSG sediment mixtures for different *UCS* values.

When clay content is 10%–20%, then

$$m_o = 0.0102; m_1 = -9.7657; m_2 = -0.0914;$$
$$m_3 = 0.3385 \quad (\text{adjusted } R^2 = 0.844)$$

and when clay content is 30%–50%, then

$$m_o = 0.0003; m_1 = -9.5363; m_2 = -0.3789;$$
$$m_3 = 0.6566 \quad (\text{adjusted } R^2 = 0.808)$$

For scour depths at the wake of the pier it was found that

$$\frac{d_{cpw}}{d_{sp}} = F_{pw} \tag{17a}$$

where F_{pw} = functional cohesion parameter for CG and CSG sediment mixtures, which is given by

$$F_{pw} = n_o[(1 + P_c)^{n_1}(1 + UCS_*)^{n_2}(t_*)^{n_3}] \tag{17b}$$

When clay content is 10%–20%, then

$$n_o = 0.004; n_1 = -3.577; n_2 = -0.238;$$
$$n_3 = 0.342 \quad (\text{adjusted } R^2 = 0.852)$$

and when clay content is 30%–50%, then

$$n_o = 0.00001; n_1 = -8.715; n_2 = -0.232;$$
$$n_3 = 0.7513 \quad (\text{adjusted } R^2 = 0.808)$$

The goodness of fit between calculated and observed values of scour depth was analyzed by the same parameters as considered and described by Jain and Kothyari (2009) and Lodhi et al. (2016), viz., discrepancy ratio (R_i), mean discrepancy ratio ($\bar{R}_i$),

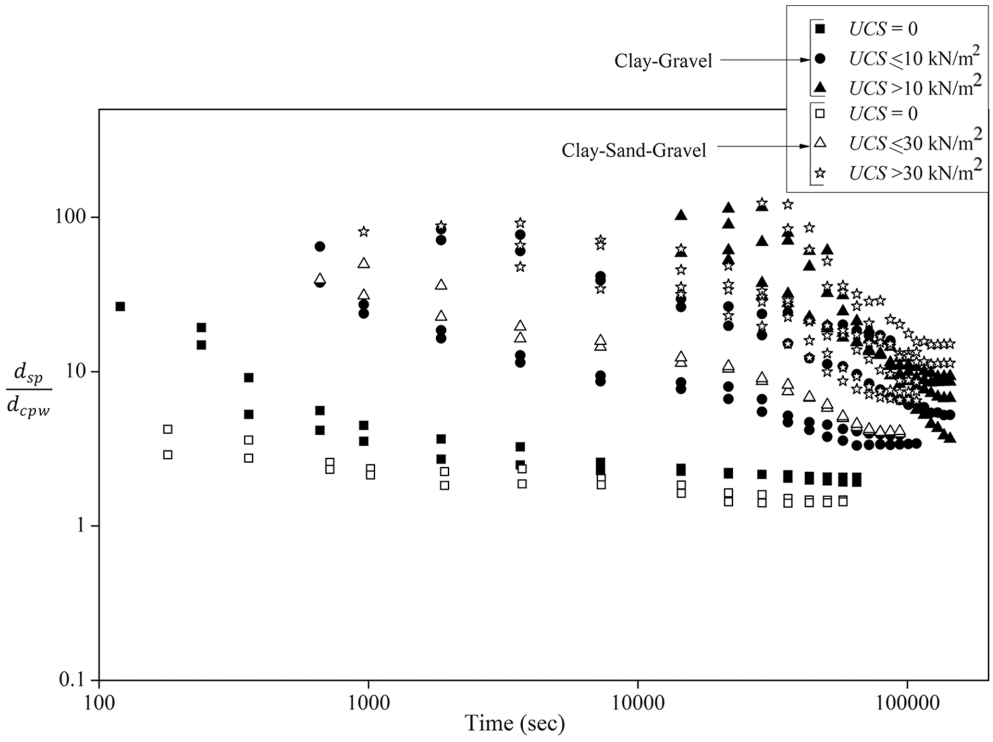

Fig. 10. Temporal variation of dimensionless scour depth at the wake of the pier in CG and CSG sediment mixtures for different *UCS* values.

Table 4. Comparison, in terms of mean discrepancy ratio ($\bar{R}_i$), difference-based average discrepancy ratio ($\bar{R}_d$), standard deviation of estimate (σ), logarithm-based standard deviation of estimate (σ_a), difference-based standard deviation of estimate (σ_d), and logarithm-ratio-based average discrepancy ratio ($\bar{D}_a$), between observed and computed values of scour depth at the sides and the wake of piers founded in CG and CSG sediment mixtures

Scour depth region	Percent of data-points in the ranges based on discrepancy ratio (R_i)									Number of data sets N
	0.75–1.25	0.5–2.0	0.33–3	$\bar{R}_i$	$\bar{R}_d$	σ	σ_a	σ_d	$\bar{D}_a$	
Side	52.57	92.57	99.42	1.1134	0.1134	0.4309	0.1551	0.01459	0.01828	350
Wake	59.40	95.22	99.70	1.0334	0.0335	0.3981	0.1483	0.0106	−0.01242	335

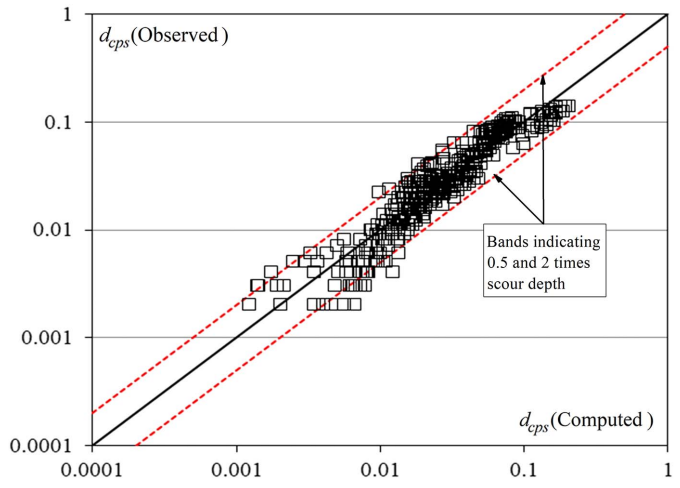

Fig. 11. Comparison of observed versus computed scour depth at the sides of the pier.

difference-based average discrepancy ratio ($\bar{R}_d$), logarithm-ratio-based average discrepancy ratio ($\bar{D}_a$), standard deviation of estimate (σ), and the difference-based (σ_d) and logarithm-based (σ_a) standard deviation of estimate. The results in terms of the preceding parameters for the comparison between calculated and observed values of scour depth at the pier sides and its wake region founded in CG and CSG sediment mixtures are given in Table 4.

The comparisons between observed and computed values of scour depths through Eqs. (16) and (17) are shown in Figs. 11 and 12, respectively. From these figures, it is observed that the proposed relationships yielded good outcomes with experimental data and around 92.57% of the data sets at the sides and 95.22% of the data sets at the wake of the pier lies under maximum error fold lines, as can be seen in Figs. 11 and 12. The scattering of data in Figs. 11 and 12 illustrates acceptable regarding parallel results stated by Kothyari et al. (2014) for pier scour, Lodhi et al. (2016, 2018) for scour around submerged and partially submerged spur dikes, and Jain and Kothyari (2009, 2010) for sediment transport in the case of sediment mixture beds prepared with CG and CSG.

Concusions

Laboratory experiments were conducted to study the influence of cohesion on scour depth around bridge piers founded in CG and CSG sediment mixtures. Firstly, experiments conducted with cohesionless sediment revealed that the initiation of scour started from the sides of the pier immediately after the experimental run started. The scour hole extended toward the pier nose where the maximum

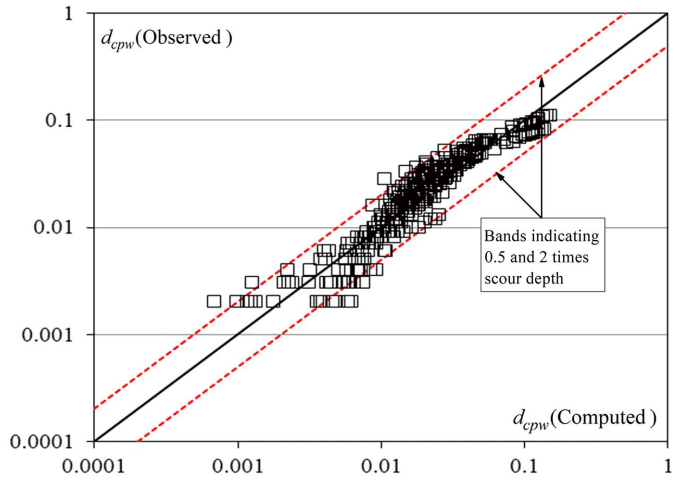

Fig. 12. Comparison of observed versus computed scour depth at the wake of the pier.

scour depth was observed at the equilibrium stage. In the case of the experiments conducted with CG and CSG sediment mixtures, scour started from the sides of the pier, at a point where separation of flow occurred, and, typically, the maximum depth of scour at the equilibrium stage was still observed at the sides of the pier. From the experiments it was found that the clay content and unconfined compressive strength are strongly influential parameters on the scour depth at piers founded in CG and CSG sediment mixtures. Specifically, the tendency of cohesive sediment mixtures to resist the erosion increases with increasing the clay content and *UCS*. This effect is more pronounced in CSG mixtures than in CG. New relationships [i.e., Eqs. (16) and (17)] are proposed to predict the scour depth at the sides and the wake of cylindrical pier embedded into CG and CSG sediment mixtures. These equations highlight the governing effects of the percent of clay, P_c, and the dimensionless unconfined compressive strength, UCS_*, on local scour processes at piers in cohesive soils. The comparison between computed and observed scour depth is depicted in Figs. 11 and 12. It was found that the proposed relationships yielded satisfactory outcomes with maximum error of two folds for 92.57% of the total data for scour depth at the sides and 95.22% of the total data for scour depth at the wake of the pier.

Limitations

The present study is confined under clear-water scour conditions. Two cylindrical piers having diameter of 8.9 and 11.52 cm, respectively, were tested. The cohesive sediment mixtures were prepared using equal proportion (by weight) of sand and gravel mixed with varying percentages of clay (10% to 50% with increments of 10%). The experiments were conducted with uniform gravel and uniform sand having median grain size of 2.7 and 0.24 mm, respectively. All experiments were performed with only one type of clay, viz., clay with high compressibility.

Data Availability Statement

All data, models, and code generated or used during the study appear in the published article.

Acknowledgments

This paper is part of the Ph.D. research work of A. S. Lodhi, conducted at the Civil Engineering Department, Indian Institute of Technology, Roorkee, India under the guidance of late Prof. U. C. Kothyari. The authors are thankful to Prof. U. C. Kothyari for choosing a research problem on a current burning issue and providing excellent guidance and painstaking efforts throughout the present research work.

Notation

The following symbols are used in this paper:

B = flume width (m);
CG = clay–gravel;
CSG = clay–sand–gravel;
C_u = cohesion (kN/m^2);
C_* = cohesion in dimensionless form;
D = pier diameter (m);
$\bar{D}_a$ = logarithm-ratio-based discrepancy ratio between observed and computed values;
D_* = grain size dimensionless form;
d_a = weighted arithmetic mean diameter of prepared CG and CSG mixture (m);
d_c = instantaneous scour depth in cohesive sediment (m);
d_{cpm} = maximum depth of scour around pier in cohesive sediment (m);
d_{cps} = instantaneous scour depth at the sides of the pier in cohesive sediment mixture (m);
d_{cpw} = instantaneous scour depth at the wake of the pier in cohesive sediment mixture (m);
d_{pm} = maximum depth of scour around pier in noncohesive sediment (m);
d_s = instantaneous scour depth in noncohesive sediment (m);
d_{sp} = calculated instantaneous scour depth in cohesionless sediment at pier under similar flow conditions (m);
d_* = dimensionless depth of scour in noncohesive sediment;
d_{50} = median particle size (m);
d_{84} = sediment size for which 84% by weight of the material is finer (m);
e = void ratio;
F_d = densimetric particle Froude number;
$F_{d\beta}$ = densimetric particle Froude number for incipient sediment entrainment at pier;
F_{di} = densimetric particle Froude number for incipient sediment entrainment in the approach channel;
F_{ps} = parameter related to the cohesion of CG and CSG mixtures at the sides of the pier;
F_{pw} = parameter related to the cohesion of CG and CSG mixtures at the wake of the pier;
g = gravitational acceleration (m/s^2);
g' = relative gravitational acceleration (m/s^2);
h = approach flow depth (m);
LL = liquid limit (%);
N = total number of data;
OMC = optimum moisture content (%);
P_c = percentage of clay (%);
PI = plasticity index (%);
PL = plastic limit (%);
$\bar{R}_d$ = difference-based average discrepancy ratio;

R_h = hydraulic radius (m);
$\overline{R_i}$ = mean discrepancy ratio;
S_o = bed slope of flume;
T = time parameter (s);
t_* = dimensionless time;
U_o = approaching flow velocity (m/s);
UCS = unconfined compressive strength (kN/m^2);
UCS_* = unconfined compressive strength of cohesive sediment mixture in dimensionless form;
u = approaching velocity of flow (m/s);
W = antecedent moisture content (%);
W_{r*} = moisture content required to saturate the soil sample (%);
$\hat{w}$ = ratio of actual to Proctor's optimum molding water content;
XRD = X-ray diffraction;
z_R = reference length (m);
$\beta = D/B$ = element obstruction;
ϕ_c = angle of friction of cohesive sediment (degrees);
ϕ_{sh} = angle of internal friction of noncohesive sediment (degrees);
ϕ_* = internal friction for cohesive sediment mixture in dimensionless form;
γ_d = dry density (kN/m^3);
γ_s = specific weight of sediment (kN/m^3);
γ_w = specific weight of water (kN/m^3);
σ = standard deviation of estimate;
σ_a = logarithm-based standard deviation of estimate;
σ_d = difference-based standard deviation of estimate;
σ_g = sediment gradation; and
σ_g' = sediment gradation of sediment mixtures.

References

Ansari, S. A., U. C. Kothyari, and K. G. Ranga Raju. 2002. "Influence of cohesion on scour around bridge piers." *J. Hydraul. Res.* 40 (6): 717–729. https://doi.org/10.1080/00221680209499918.

Ansari, S. A., U. C. Kothyari, and K. G. Ranga Raju. 2003. "Influence of cohesion on scour under submerged circular vertical jet." *J. Hydraul. Eng.* 129 (12): 1014–1019. https://doi.org/10.1061/(ASCE)0733-9429(2003)129:12(1014).

Azamathulla, H. M. 2012. "Gene expression programming for prediction of scour depth downstream of sills." *J. Hydrol.* 460–461 (Aug): 156–159. https://doi.org/10.1016/j.jhydrol.2012.06.034.

Azamathulla, H. M., A. A. Ghani, N. A. Zakaria, and A. Guven. 2010. "Genetic programming to predict bridge pier scour." *J. Hydraul. Eng.* 136 (3): 165–169. https://doi.org/10.1061/(ASCE)HY.1943-7900.0000133.

Barbhuiya, A. K., and T. Chakma. 2012. "Effect of consolidation on local scour around bridge pier in cohesive soil." *Int. J. Eng. Res. Technol.* 1 (7): 1–9.

Brandimarte, L., A. Montanari, J. L. Briaud, and P. D'Odorico. 2006. "Stochastic flow analysis for predicting scour of cohesive soils." *J. Hydraul. Eng.* 132 (5): 493–500. https://doi.org/10.1061/(ASCE)0733-9429(2006)132:5(493).

Briaud, J. L., H. C. Chen, K. W. Kwak, S. W. Han, and F. C. K. Ting. 2001. "Erosion function apparatus for scour rate predictions." *J. Geotech. Geoenviron. Eng.* 127 (2): 105–113. https://doi.org/10.1061/(ASCE)1090-0241(2001)127:2(105).

Briaud, J. L., F. C. K. Ting, S. C. Chen, R. Gudavalli, S. Perugu, and G. Wei. 1999. "SRICOS: Prediction of scour rate in cohesive soils at bridge piers." *J. Geotech. Geoenviron. Eng.* 125 (4): 237–246. https://doi.org/10.1061/(ASCE)1090-0241(1999)125:4(237).

Chaudhuri, S., and K. Debnath. 2013. "Observations on initiation of pier scour and equilibrium scour hole profiles in cohesive sediments." *ISH J. Hydraul. Eng.* 19 (1): 27–37. https://doi.org/10.1080/09715010.2012.749011.

Debnath, K., and S. Chaudhuri. 2010a. "Bridge pier scour in clay-sand mixed sediments at near-threshold velocity for sand." *J. Hydraul. Eng.* 136 (9): 597–609. https://doi.org/10.1061/(ASCE)HY.1943-7900.0000221.

Debnath, K., and S. Chaudhuri. 2010b. "Laboratory experiments on local scour around cylinder for clay and clay-sand mixed beds." *Eng. Geol.* 111 (1–4): 51–61. https://doi.org/10.1016/j.enggeo.2009.12.003.

Dey, S., A. Helkjær, B. M. Sumer, and J. Fredsøe. 2011. "Scour at vertical piles in sand-clay mixtures under waves." *J. Waterway, Port, Coastal, Ocean Eng.* 137 (6): 331–334. https://doi.org/10.1061/(ASCE)WW.1943-5460.0000095.

Ettema, R., B. W. Melville, and B. Barkdoll. 1998. "Scale effect in pier-scour experiments." *J. Hydraul. Eng.* 124 (6): 639–642. https://doi.org/10.1061/(ASCE)0733-9429(1998)124:6(639).

Hamidifar, H., and M. H. Omid. 2017. "Local scour of cohesive beds downstream of a rigid apron." *Can. J. Civ. Eng.* 44 (11): 935–944. https://doi.org/10.1139/cjce-2016-0398.

Hanson, G. J., and S. L. Hunt. 2006. "Lessons learned using laboratory JET method to measure soil erodibility of compacted soils." *Appl. Eng. Agric.* 23 (3): 305–312. https://doi.org/10.13031/2013.22686.

Hosny, H. M. 1995. "Experimental study of local scour around circular bridge piers in cohesive soils." Ph.D. thesis, Dept. of Civil Engineering, Colorado State Univ.

Jain, R. K., and U. C. Kothyari. 2009. "Cohesion influences on erosion and bed load transport." *Water Resour. Res.* 45 (6): W06410. https://doi.org/10.1029/2008WR007044.

Jain, R. K., and U. C. Kothyari. 2010. "Influence of cohesion on suspended load transport of non-uniform sediments." *J. Hydraul. Res.* 48 (1): 33–43. https://doi.org/10.1080/00221681003696317.

Kamojjala, S., N. P. Gattu, A. C. Parola, and D. J. Hagerty. 1995. "Analysis of 1993 upper Mississippi flood highway infrastructure damage." In Vol. 2 of *Proc., 1st Int. Conf. on Water Resources Engineering*, 1061–1065. New York: ASCE.

Kand, C. V. 1993. Vol. 9 and 10 of *Pier scour in sand, clay and boulders*. New Delhi, India: Bridge Engineering.

Kho, K. T. 2004. "An experimental study of local scour around circular bridge piers in cohesive soils." Ph.D. thesis, School of Civil Engineering and Geosciences, Univ. of Newcastle Upon Tyne.

Kothyari, U. C. 2007. "Indian practice on estimation of scour around bridge piers: A comment." *Sadhana* 32 (3): 187–197. https://doi.org/10.1007/s12046-007-0017-7.

Kothyari, U. C., W. H. Hager, and G. Oliveto. 2007. "Generalized approach for clear-water scour at bridge foundation elements." *J. Hydraul. Eng.* 133 (11): 1229–1240. https://doi.org/10.1061/(ASCE)0733-9429(2007)133:11(1229).

Kothyari, U. C., and R. K. Jain. 2008. "Influence of cohesion on the incipient motion condition of sediment mixtures." *Water Resour. Res.* 44 (4): W04410. https://doi.org/10.1029/2007WR006326.

Kothyari, U. C., and R. K. Jain. 2010a. "Erosion characteristics of cohesive sediment mixtures." In *Proc., Int. Conf. on Fluvial Hydraulics: River Flow 2010*, edited by A. Dittrich, K. Koll, J. Aberle, and P. Geisenhainer, 815–820. Karlsruhe, Germany: Bundesanstalt für Wasserbau.

Kothyari, U. C., and R. K. Jain. 2010b. "Experimental and numerical investigations on degradation of channel bed of cohesive sediment mixtures." *Water Resour. Res.* 46 (12): W12534. https://doi.org/10.1029/2010WR009184.

Kothyari, U. C., A. Kumar, and R. K. Jain. 2014. "Influence of cohesion on river bed scour in the wake region of piers." *J. Hydraul. Eng.* 140 (1): 1–13. https://doi.org/10.1061/(ASCE)HY.1943-7900.0000793.

Kumar, A. 2011. "Scour around circular piers founded in clay-sand-gravel sediment mixtures." Ph.D. thesis, Dept. of Civil Engineering, Indian Institute of Technology.

Kurdistani, S. M., and S. Pagliara. 2017. "Experimental study on cross-vane scour morphology in curved horizontal channels." *J. Irrig. Drain. Eng.* 143 (7): 04017013. https://doi.org/10.1061/(ASCE)IR.1943-4774.0001183.

Link, O., K. Klischies, G. Montalva, and S. Dey. 2013. "Effects of bed compaction on scour at piers in sand-clay mixtures." *J. Hydraul. Eng.* 139 (9): 1013–1019. https://doi.org/10.1061/(ASCE)HY.1943-7900.0000762.

Lodhi, A. S., R. K. Jain, and P. K. Sharma. 2016. "Influence of cohesion on scour around submerged dike founded in clay–sand–gravel mixtures." *ISH J. Hydraul. Eng.* 22 (1): 70–87. https://doi.org/10.1080/09715010.2015.1075916.

Lodhi, A. S., R. K. Jain, P. K. Sharma, and N. Karna. 2018. "Influence of cohesion on scour at wake of partially submerged spur dikes in cohesive sediment mixtures." *ISH J. Hydraul. Eng.* 27 (2): 123–134. https://doi.org/10.1080/09715010.2018.1525325.

Lodhi, A. S., P. K. Sharma, R. K. Jain, and N. Karna. 2014. "Temporal evolution of clear water bridge pier scour." In *Proc., Int. Civil Engineering Symp., ICES' 2014*, 252–260. Chennai, India: VIT Vellore.

Mazurek, K. A. 2001. "Scour of clay by jets." Ph.D. dissertation, Dept. of Civil and Environmental Engineering, Univ. of Alberta.

Mazurek, K. A., N. Rajaratnam, and D. C. Sego. 2001. "Scour of cohesive soil by submerged circular turbulent impinging jets." *J. Hydraul. Eng.* 127 (7): 598–606. https://doi.org/10.1061/(ASCE)0733-9429(2001)127:7(598).

Molinas, A., S. Jones, and M. Hosny. 1999. "Effects of cohesive material properties on local scour around piers." *Transp. Res. Rec.* 1690 (1): 164–174. https://doi.org/10.3141/1690-19.

Oliveto, G., and W. H. Hager. 2002. "Temporal evolution of clear-water pier and abutment scour." *J. Hydraul. Eng.* 128 (9): 811–820. https://doi.org/10.1061/(ASCE)0733-9429(2002)128:9(811).

Oliveto, G., and W. H. Hager. 2005. "Further results to time-dependent local scour at bridge elements." *J. Hydraul. Eng.* 131 (2): 97–105. https://doi.org/10.1061/(ASCE)0733-9429(2005)131:2(97).

Oliveto, G., and W. H. Hager. 2014. "Morphological evolution of dune-like bed forms generated by bridge scour." *J. Hydraul. Eng.* 140 (5): 06014009. https://doi.org/10.1061/(ASCE)HY.1943-7900.0000853.

Pagliara, S., and M. Palermo. 2011. "Effect of stilling basin geometry on clear water scour morphology downstream of a block ramp." *J. Irrig. Drain. Eng.* 137 (9): 593–601. https://doi.org/10.1061/(ASCE)IR.1943-4774.0000331.

Pandey, M., H. M. Azamathulla, S. Chaudhuri, J. H. Pu, and H. Pourshahbaz. 2020a. "Reduction of time-dependent scour around piers using collars." *Ocean Eng.* 213 (Oct): 107692. https://doi.org/10.1016/j.oceaneng.2020.107692.

Pandey, M., W. H. Lam, Y. Cui, M. A. Khan, U. K. Singh, and Z. Ahmad. 2019. "Scour around spur dike in sand-gravel mixture bed." *Water* 11 (7): 1417. https://doi.org/10.3390/w11071417.

Pandey, M., G. Oliveto, J. H. Pu, P. K. Sharma, and C. S. P. Ojha. 2020b. "Pier scour prediction in non-uniform gravel beds." *Water* 12 (6): 1696. https://doi.org/10.3390/w12061696.

Pandey, M., P. K. Sharma, Z. Ahmad, U. K. Singh, and N. Karna. 2018. "Three-dimensional velocity measurements around bridge piers in gravel bed." *Mar. Georesour. Geotechnol.* 36 (6): 663–676. https://doi.org/10.1080/1064119X.2017.1362085.

Pandey, M., M. Valyrakis, M. Qi, A. Sharma, and A. S. Lodhi. 2020c. "Experimental assessment and prediction of temporal scour depth around a spur dike." *Int. J. Sediment Res.* 36 (1): 17–28. https://doi.org/10.1016/j.ijsrc.2020.03.015.

Parola, A. C., D. J. Hagerty, D. S. Mueller, B. W. Melville, G. Parker, and J. S. Usher. 1997. "The need for research on scour at bridge crossings." In Vol. 1 of *Proc., 27th Congress of the Int. Association for Hydraulic Research*, 124–129. San Francisco. Water Resources Engineering Hydraulics.

Peerless, S. J. 1967. *Basic fluid mechanics*. Oxford, NY: Pergamon Press.

Pourshahbaz, H., S. Abbasi, M. Pandey, J. H. Pu, P. Taghvaei, and N. Tofangdar. 2020. "Morphology and hydrodynamics numerical simulation around groynes." *ISH J. Hydraul. Eng.* 1–9. https://doi.org/10.1080/09715010.2020.1830000.

Pu, J. H., M. Pandey, and P. R. Hanmaiahgari. 2020. "Analytical modelling of sidewall turbulence effect on streamwise velocity profile using 2D approach: A comparison of rectangular and trapezoidal open channel flows." *J. Hydro-environ. Res.* 32 (Oct): 17–25. https://doi.org/10.1016/j.jher.2020.06.002.

Ram Babu, M., S. N. Rao, and V. Sundar. 2002. "A simplified instrumentation for measuring scour in silty clay around a vertical pile." *Appl. Ocean Res.* 24 (6): 355–360. https://doi.org/10.1016/S0141-1187(03)00027-0.

Robinson, K. M., and G. J. Hanson. 1995. "Large-scale headcut erosion testing." *Trans. ASABE* 38 (2): 429–434. https://doi.org/10.13031/2013.27849.

Singh, R. K., M. Pandey, J. H. Pu, S. Pasupuleti, and V. G. K. Villuri. 2020. "Experimental study of clear-water contraction scour." *Water Supply* 20 (3): 943–952. https://doi.org/10.2166/ws.2020.014.

Singh, U. K., Z. Ahmad, A. Kumar, and M. Pandey. 2019. "Incipient motion for gravel particles in cohesionless sediment mixtures." *Iran. J. Sci. Technol. Trans. Civ. Eng.* 43 (2): 253–262. https://doi.org/10.1007/s40996-018-0136-x.

Ting, F. C. K., J. -L. Briaud, H. C. Chen, R. Gudavalli, S. Perugu, and G. Wei. 2001. "Flume tests for scour in clay at circular piers." *J. Hydraul. Eng.* 127 (11): 969–978. https://doi.org/10.1061/(ASCE)0733-9429(2001)127:11(969).